



## Improvement of a Magnus VAWT Based on Numerical Simulation using a Fixed Blade

Ainura Dyusembaeva<sup>1,2</sup>, Nazgul Tanasheva<sup>1,2</sup>, Indira Sarzhanova<sup>1,2</sup>, Asem Bakhtybekova<sup>1,2,\*</sup>, Akmaral Tleubergenova<sup>1,2</sup>, Nurgul Abdirova<sup>1</sup>, Nurgul Shuyushbayeva<sup>1,3</sup>

<sup>1</sup> Department of Engineering Thermophysics, Karaganda Buketov University, Karaganda, Kazakhstan

<sup>2</sup> Scientific research center "Alternative Energy", Karaganda Buketov University, Karaganda, Kazakhstan

<sup>3</sup> Department of Mathematics, Physics and Computer Science, Sh. Ualikhanov Kokshetau STATE University, Kokshetau 020000, Kazakhstan

### ARTICLE INFO

#### Article history:

Received 10 October 2024

Received in revised form 14 November 2024

Accepted 18 December 2024

Available online 31 January 2025

#### Keywords:

Magnus; wind turbine; fixed blades; cylinder; numerical simulation

### ABSTRACT

Magnus wind turbines have a wide range of advantages ranging from generating energy at low wind speeds to adapting to any wind direction. However, the cylindrical blades themselves have high drag and low lift. The aim of the work is to study the addition of a fixed blade to the cylindrical blades of a wind turbine to improve the efficiency of the entire wind turbine. The paper presents a numerical study of the lifting force and drag force of a wind turbine, as well as the blades themselves, averaged over time from the air flow velocity and the number of revolutions. Using the averaging method of the Navier-Stokes equations RANS (Reynolds-averaged Navier–Stokes), numerical results were obtained showing the efficiency of the installation starting from 3 m/s, i.e. low wind speeds. It is determined that the use of adding a fixed blade to a rotating cylinder gives an increase in the value of the lifting force from 40-55% and power factor of the wind turbine by almost 1.5-1.7 times due to the regulation and reduction of the disruption of vortices behind the rotating cylinder. The effect of the plate on the velocity and pressure field is illustrated. The results obtained are useful when designing real experimental installations.

## 1. Introduction

Wind energy is one of the most efficiently developing alternative technologies for the production of electricity. According to data by International Energy Agency [1], the total installed capacity for wind power generation reached 2,100 TWh, almost an increase of 265 TWh (an increase of 14%). In terms of growth, wind energy is second only to solar energy. In 2022, China is the leader in global wind energy growth.

The creation and research of effective designs of wind turbines designed for low wind speeds, especially for decentralized power supply of remote areas, urban facilities, is extremely necessary for the development of wind energy in cities [2]. One of the representatives of wind turbines is installations with a vertical axis of rotation (VAWT). The main advantage of VAWT from HAWT

\* Corresponding author.

E-mail address: [asem.alibekova@inbox.ru](mailto:asem.alibekova@inbox.ru) (Asem Bakhtybekova)

<https://doi.org/10.37934/cfdl.17.7.98112>

(Horizontal-axis wind turbine) is the extraction of energy regardless of the wind direction. However, there is one drawback in the form of negative torque resulting in a decrease in wind energy utilization. To solve this problem, it is necessary to add deflector concentrators, as well as optimize the shape of the blades by modifying their profiles [3]. Also, to increase the efficiency and reliability of the entire installation, it is necessary to use simulation analysis [4].

To increase the efficiency of the VAWT, various approaches are proposed: the addition of deflectors and guiding devices [5-7] to control the flow of air around the turbine, which helps to reduce the negative impact of turbulence and increase lift; optimizing the shape of the blades [8-10] by changing their geometry, including curvature or the addition of protrusions, which improves aerodynamic properties and increases the power factor; the use of combined blades [11-13], in which the combination of rotating elements with fixed ones leads to an improvement in aerodynamic characteristics by reducing vortex formation.

To increase the power output of the installation, Alizadeh *et al.*, [5] added a simple barrier to deflect the liquid flow from the reversible bucket of the Savonius turbine. Numerical simulation was performed using computational fluid dynamics (CFD) based on the SST (Shear Stress Transport) transition turbulence model in order to determine the optimal barrier length. The comparison results showed an increase in power output by 18% compared to traditional Savonius turbines. However, the disadvantage of these wind turbines is the low power coefficient and very high material consumption.

The research by Sewucipto *et al.*, [6] is aimed at increasing the efficiency of a Savonius type wind turbine by using a D-53° cylinder as a passive control mechanism in front of the return blade of the wind turbine. The study notes that the reduced return blade resistance created by the cylinder played a key role in improving turbine efficiency by changing flow characteristics and reducing pressure resistance. The study lacks a detailed analysis of key aerodynamic parameters such as lift coefficient (Cl) and drag coefficient (Cd). This omission limits a comprehensive understanding of how the passive control mechanism affects the aerodynamic characteristics of the turbine, which is crucial for evaluating and optimizing its overall efficiency.

Salleh *et al.*, [7] conducted a qualitative study of the effect of adding a deflector to the turbine, as well as changes in the coefficients of the longitudinal position of the retractable blade and the reflector of the returning blade. It is established that the deflector at the optimal position reduces the negative torque by excluding the flow from entering the low-pressure area. In operation, the drag force on the returning blade creates a negative torque, which reduces the effects of adding a deflector and this issue has not been fully studied.

It is important to determine the most optimal configuration of the Savonius vertical axis wind turbine, which provides the best performance with high self-starting capability. Saad *et al.*, [8] investigated the effect of several design parameters on the performance of a Savonius wind turbine. An interesting fact is the use of new estimation methods based on the characteristics of the pressure and flow fields. However, there are no data on the effect of changes in design features on the aerodynamic forces arising from the flow around a wind turbine.

Li *et al.*, [9] conducted experimental studies of wind turbines with two vertical axes of rotation (VAWT) in real urban conditions across a number of large cities. The results showed that wind turbines with two vertical axes of rotation have little effect on the output power of the VAWT compared to an isolated VAWT at low wind speeds in urban conditions. These studies are important for designing wind turbines in large cities. Nevertheless, the results of mathematical modelling would improve the significance of the results obtained.

Yan *et al.*, [10] performed numerical modelling of the influence of the leading-edge protrusion for a vertical axis wind turbine (VAWT) using nonstationary Reynolds-Averaged-Navier-Stokes

(URANS) and implicit large vortex modelling (ILES). An interesting fact is that the amplitude of the protrusions is more important than the wavelength to improve aerodynamic performance. However, the data obtained must be compared with laboratory data in order to obtain a complete picture of the effect of the leading-edge protrusion.

One of the types of turbines operating at low wind speeds are Magnus wind turbines with cylindrical blades. Many research articles [11-13] are devoted to the study of the aerodynamic characteristics of Magnus wind turbines with various blade configurations. Magnus wind turbines have the advantages of being used in a wider range of wind speeds: from 2 to 40 m/s versus 5-25 m/s for conventional blade installations. However, most of these installations have a disadvantage in the form of vortices at the ends of the cylinders, leading to a decrease in power output and aerodynamic noise. Additionally, the cylindrical blades themselves have low lift and high drag forces, which affects the output power. A method is known by Zhao [14] to suppress the formation of vortices behind a rotating cylinder, in the form of adding control plates at a certain angle to the cylinder, which in turn significantly reduces the drag force.

Simulation is crucial for advancing the design and optimization of wind turbines, as highlighted in the work by Bahambary *et al.*, [15]. They emphasize that computational fluid dynamics (CFD) simulations play an essential role in modelling wind turbines, enabling researchers to analyse aerodynamic behaviour effectively.

Eydi *et al.*, [16] performed a numerical study of the addition of an arc plate to the back of a round cylinder in a turbulent flow regime with a Reynolds number of 22,000. It is determined that the addition of arc plates reduces the noise level and drag coefficient.

In another study, Kimura *et al.*, [17] conducted a numerical investigation on a Magnus wind turbine with a vertical axis of rotation. They found that adding protective plates to both ends of the cylinder blades, along with curved wings along the blades, was the most effective way to suppress vortices at the blade ends.

Sedaghat *et al.*, [18] conducted a numerical study of new circulating aerodynamic profiles for use in the blades of Magnus wind turbines, suggesting replacing traditional rotating cylinders with circulating aerodynamic profiles with a moving surface. Their results showed a significant increase in the ratio of lift to resistance, reaching values above 278, which indicates the potential to increase the efficiency of such turbines. However, their work has drawbacks: low overall efficiency of the system due to the difficulties of implementing the moving surface of the blade and significant energy costs for its actuation, as well as technical difficulties in the manufacture of such blades.

One of the methods to increase the energy efficiency of a wind turbine is to modify the surface of the blades by increasing its roughness. Marzuki *et al.*, [19] conducted an experimental study of the effect of surface roughness on the operation of a Magnus wind turbine using sandblasting of cylindrical blades. The results showed that a rough surface can increase the torque coefficient of a turbine by four times compared to a smooth surface, as well as reduce the minimum wind speed required to start the rotor. However, the disadvantages of the work are that there are no aerodynamic coefficients for a more complete analysis and detailed understanding of the behaviour of the turbine. Surface roughness also improves interaction with the boundary layer and is effective for increasing lift under certain conditions, but can lead to accelerated surface wear.

Also, an important indicator for evaluating the efficiency of a wind turbine is the power coefficient ( $C_p$ ) [20]. In the work, Limpot *et al.*, [21] investigated the performance of a Magnus-type vertical axis wind turbine (VAWT) exposed to typhoon wind speeds. It is determined that when modelling  $C_p = 0.58$  with a gear ratio of 2, which is overestimated and almost close to  $C_p$  for ideal wind turbines [22]. When calculating, it is necessary to take into account the power of the cylinders and the wind wheel itself.

Despite the significant amount of research devoted to improving the aerodynamic characteristics of Magnus wind turbines, there is insufficient research on the use of combined structures including fixed elements to increase turbine efficiency. Previous studies have focused on traditional solutions such as modification of rotating cylinders and the use of various aerodynamic profiles aimed at reducing drag and increasing lift. However, limited attention has been paid to the integration of fixed blades, which can contribute to an additional increase in aerodynamic efficiency by stabilizing the flow and reducing vortex formation. The present study aims to eliminate this gap by presenting the results of numerical simulation of a wind turbine with combined blades, including an assessment of their impact on aerodynamic parameters and performance at low wind speeds. The data obtained expand the existing scientific knowledge base and can serve as a basis for further experimental research and development of improved designs of wind turbines.

## 2. Materials and Methods

### 2.1 Model of Wind Turbine with Combined Blades

The authors of the work created a model of a wind turbine with combined blades for numerical research (Figure 1).

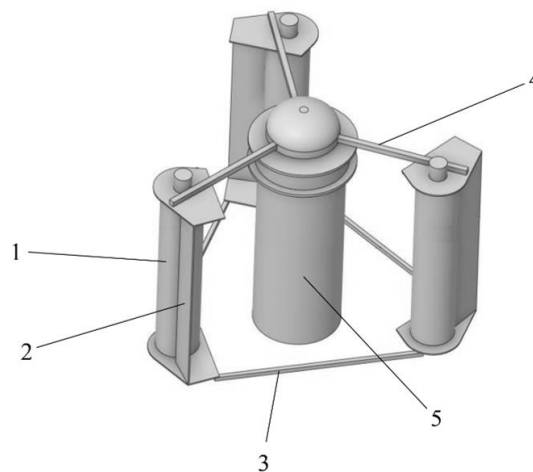


**Fig. 1.** Wind turbine with combined blades: 1 – cylinder rotating around its axis; 2 – fixed blade; 3, 4 – retaining rods; 5 – support of the wind turbine

The model of a wind turbine is a wind wheel containing 3 combined blades, consisting of rotating cylinders (1) with a diameter of 0.15 m and a height of 0.69 m and a fixed blade (2) with a thickness of 0.005 m, a height of 0.715 m and a width of 0.1182 m.

The combined blades are interconnected by retaining upper rods (4), whose cross section is 0.03 m·0.03 m and lower rods (3), with dimensions of 0.015 m·0.015 m. The entire wind wheel is fixed to the support of the wind turbine (5), the distance from the support to the axis of the cylinder is 0.5 m. The projections of the axes of the rotating cylinders on the horizontal plane form the vertices of a regular triangle.

## 2.2 The Difference Grid of the Model

The authors used a method for modelling turbulent flows based on solving the averaged Navier-Stokes equations (RANS).

The calculations used a difference grid containing 24555 quadrangular cells, shown in Figure 2. In the stationary region 1, Figure 2, 2,771 cells were built, in the rotating region 2, Figure 2, 17,836 cells were built, in the rotating region of the cylinder 3, Figure 2, 1,316 cells were built.

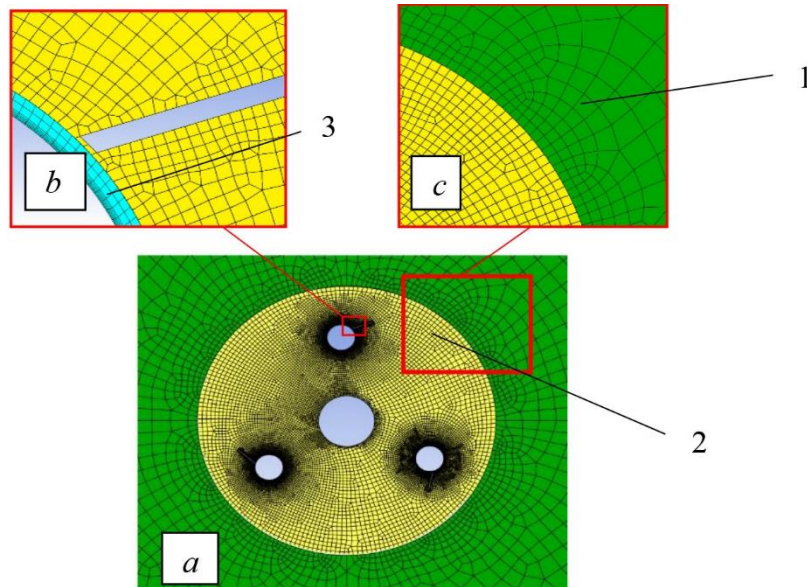


**Fig. 2.** Grid area: a – general view of the grid area; b – view of the grid in the vicinity of the rotating cylinder and blade; c – view of the grid in the vicinity of the interface, rotating and stationary areas.

The mesh was thickened near the walls of the cylinders, blades and supports. During the numerical simulation, a number of assumptions were made and certain limitations were accepted, which must be taken into account when interpreting the results. The use of the RANS (Reynolds-Averaged Navier-Stokes) model assumes averaging of the turbulent flow characteristics, which may reduce the accuracy of the description of non-stationary and small-scale vortices. In addition, the calculations were carried out in a two-dimensional formulation, which simplifies the geometry and does not take into account spatial effects such as end vortices at the edges of the blades. The model also assumes an isothermal environment and does not take into account temperature changes, which may be important when analysing in real conditions. These limitations should be taken into account when extrapolating the results to real installations, since experimental studies can reveal differences in aerodynamic characteristics and turbine performance.

To describe the turbulent airflow around the wind turbine, the Reynolds-Averaged Navier-Stokes (RANS) equations are employed, providing an averaged representation of turbulent flow characteristics. The governing equations for incompressible and isothermal flow include the continuity equation and the momentum equation [11,23].

For incompressible flow, the continuity equation is expressed as Eq. (1):

$$\frac{\partial x_i}{\partial u_i} = 0 \quad (1)$$

where  $u_i$  represents the velocity components of the flow and  $x_i$  represents the spatial coordinates.

The Reynolds-averaged momentum equations for turbulent flow are given by Eq. (2):

$$\frac{\partial(\rho u_i)}{\partial t} + \frac{\partial(\rho u_i u_j)}{\partial x_j} = -\frac{\partial p}{\partial x_i} + \frac{\partial}{\partial x_j} \left( \mu \frac{\partial u_i}{\partial x_j} \right) - \frac{\partial}{\partial x_j} (\rho \overline{u_i' u_j'}) \quad (2)$$

where,  $\rho$  is the fluid density;  $P$  is the pressure;  $\mu$  is the dynamic viscosity;  $\overline{u_i' u_j'}$  are the Reynolds stresses that model the turbulent stresses arising from velocity fluctuations.

The Realizable  $k-\varepsilon$  model is applied in this study, which improves upon the standard  $k-\varepsilon$  model by imposing realizability constraints on the turbulent kinetic energy and dissipation rate. This approach enhances accuracy for complex turbulent flows, such as rotating and recirculating flows around the wind turbine's cylindrical elements [11].

The transport equation for turbulent kinetic energy  $k$  Eq. (3) is given by:

$$\frac{\partial(\rho k)}{\partial t} + \frac{\partial(\rho u_i k)}{\partial x_i} = \frac{\partial}{\partial x_j} \left[ \left( \mu + \frac{\mu_t}{\sigma_k} \right) \frac{\partial k}{\partial x_j} \right] + Pk - \rho \varepsilon \quad (3)$$

where,  $k$  is the turbulent kinetic energy;  $\mu_t$  is the turbulent viscosity;  $\sigma_k$  is the turbulent Prandtl number for  $k$ ,  $P_k$  is the production of turbulent kinetic energy;  $\varepsilon$  is the dissipation rate of turbulent kinetic energy.

The transport equation for the dissipation rate  $\varepsilon$  Eq. (4) is:

$$\frac{\partial(\rho \varepsilon)}{\partial t} + \frac{\partial(\rho u_i \varepsilon)}{\partial x_i} = \frac{\partial}{\partial x_j} \left[ \left( \mu + \frac{\mu_t}{\sigma_\varepsilon} \right) \frac{\partial \varepsilon}{\partial x_j} \right] + \rho C_1 S \varepsilon - \rho C_2 k + \frac{\varepsilon^2}{\sqrt{v \varepsilon}} \quad (4)$$

where  $\sigma_\varepsilon$  is the turbulent Prandtl number for  $\varepsilon$  epsilon,  $C_1$  and  $C_2$  are empirical constants and  $S$  is the modulus of the mean rate-of-strain tensor.

The turbulent viscosity  $\mu_t$  Eq. (5) is computed as:

$$\mu_t = \rho C_\mu \frac{k^2}{\varepsilon} \quad (5)$$

where  $C_\mu$  is a model constant.

A counter current difference scheme of the second order of accuracy in space was used. The central difference scheme was used to approximate second-order derivatives. The Coupled scheme was used to coordinate the pressure field and the velocity field. Time derivatives were resolved with the first order of accuracy. The time step was set to be  $4 \cdot 10^{-4}$  s.

The boundary conditions at the input and output of the region are shown in Table 1.

**Table 1**  
Boundary conditions at the entrance and exit to the region

Boundary conditions	
Inlet	
Type	Inlet speed
Initial pressure gauge (Pa)	0
Air flow velocity, m/s	3, 5, 7, 10, 15
Turbulence intensity (%)	5
Coefficient of turbulent viscosity	10
Outlet	
Type	Outlet pressure
Pressure gauge (Pa)	0
Reverse flow of turbulent intensity (%)	5
Coefficient of backflow of turbulent intensity (%)	10
Blade surface	
Type	Wall
Shift condition	No slipping
Periodic conditions	
Type	Rotation
The number of rotations of the blades (rpm)	315, 550, 720

Using the data in Table 1, mathematical modelling was performed.

### 2.3 Determination of Aerodynamic Coefficients

In this study, aerodynamic coefficients such as lift coefficient ( $C_l$ ), torque coefficient ( $C_q$ ), power coefficient ( $C_p$ ) and drag coefficient ( $C_d$ ) were used to evaluate the performance of the wind turbine with combined blades. These coefficients provide a detailed analysis of the aerodynamic properties and efficiency of the turbine.

Lift Coefficient ( $C_l$ ) Eq. (6):

$$C_l = \frac{L}{\frac{1}{2}\rho V^2 A} \quad (6)$$

where,  $L$  is the lift force (N),  $\rho$  is the air density ( $\text{kg/m}^3$ ),  $V$  is the incoming flow velocity (m/s),  $A$  is the reference area ( $\text{m}^2$ ), in this case, the blade area.

Drag Coefficient ( $C_d$ ) Eq. (7):

$$C_d = \frac{D}{\frac{1}{2}\rho V^2 A} \quad (7)$$

where,  $D$  is the drag force (N).

Torque Coefficient ( $C_q$ ) Eq. (8):

$$C_q = \frac{M}{\frac{1}{2}\rho V^2 AR} \quad (8)$$

where,  $M$  is the torque (N·m),  $R$  is the radius of the wind turbine (m).

Power Coefficient ( $C_p$ ) Eq. (9):

$$C_p = \frac{P}{\frac{1}{2}\rho V^3 A} \quad (9)$$

where,  $C_p$  is the mechanical power output of the turbine (W).

### 3. Results and Discussions

Figure 3 shows the air flow lines in the vicinity of the wind wheel for flow rates of 3 m/s, 9 m/s, 15 m/s and cylinder rotation speeds of 315 rpm and 720 rpm. The air flow moves from left to right. It is clearly seen that vortex zones are formed in the vicinity of the blades. An increase in the cylinder rotation speed from 315 rpm to 720 rpm for an incoming flow velocity of 3 m/s (Figure 3(a) and 3(d)) leads to more intense vortex formation, whereas at a higher flow velocity of 15 m/s, vortex formation is less pronounced (Figure 3(b) and 3(e)).

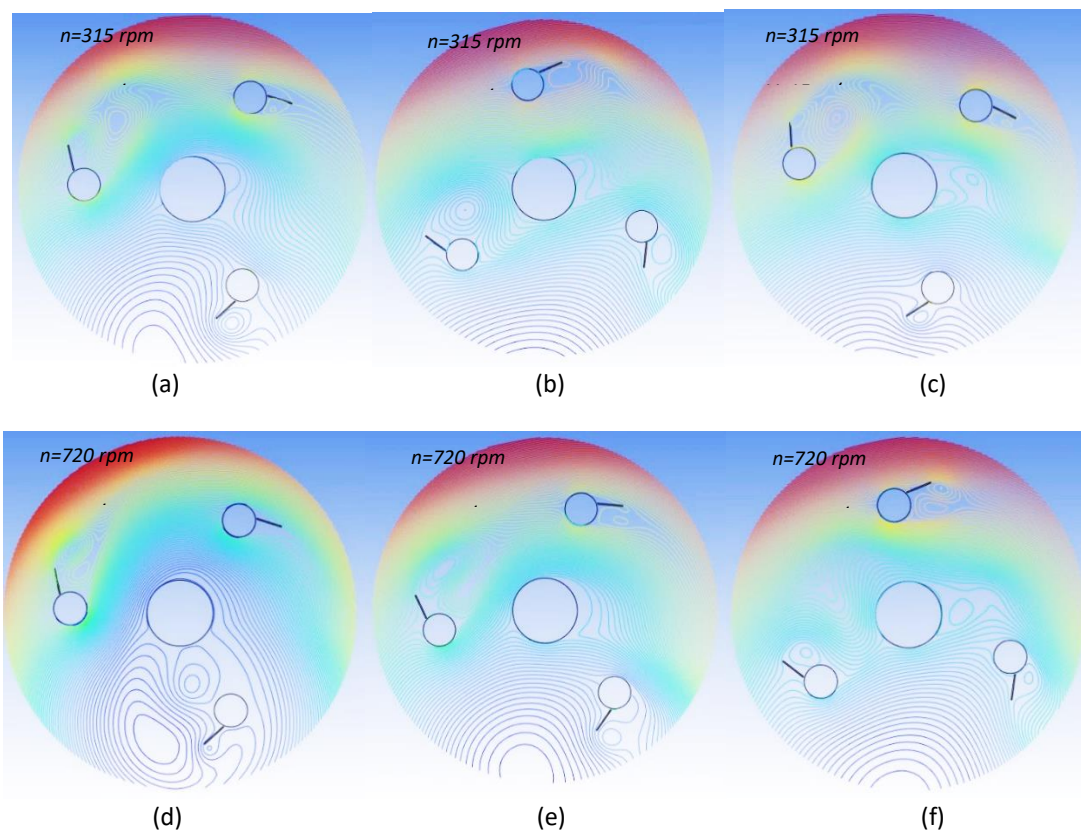


**Fig. 3.** Current lines in the vicinity of the wind wheel: (a), (b), (c) –  $n=315$  rpm, (d), (e), (f) –  $n=720$  rpm, (a), (d) –  $V=3$  m/s, (b), (e) –  $V=9$  m/s, (c), (f) –  $V=15$  m/s

As can be seen from Figure 3, vortex formation is observed behind the cylinders and behind the fixed blade - the Pocket tracks. The distributions of velocity profiles and its pulsations generally maintain symmetry relative to the axis of the cylinder. However, it is noticeable that with an increase in the rotation frequency, some deviation from symmetry takes place. The formation of large-scale vortices occurs mainly in the phase of flow acceleration.



Figure 4 shows the overpressure fields in Pascals. A value of 0 corresponds to 1 atm. An increase in the velocity of the incoming flow leads to an increase in the pressure drop on the cylinders and blades of the wind wheel. The same effect is observed with an increase in the speed of rotation of the cylinders.

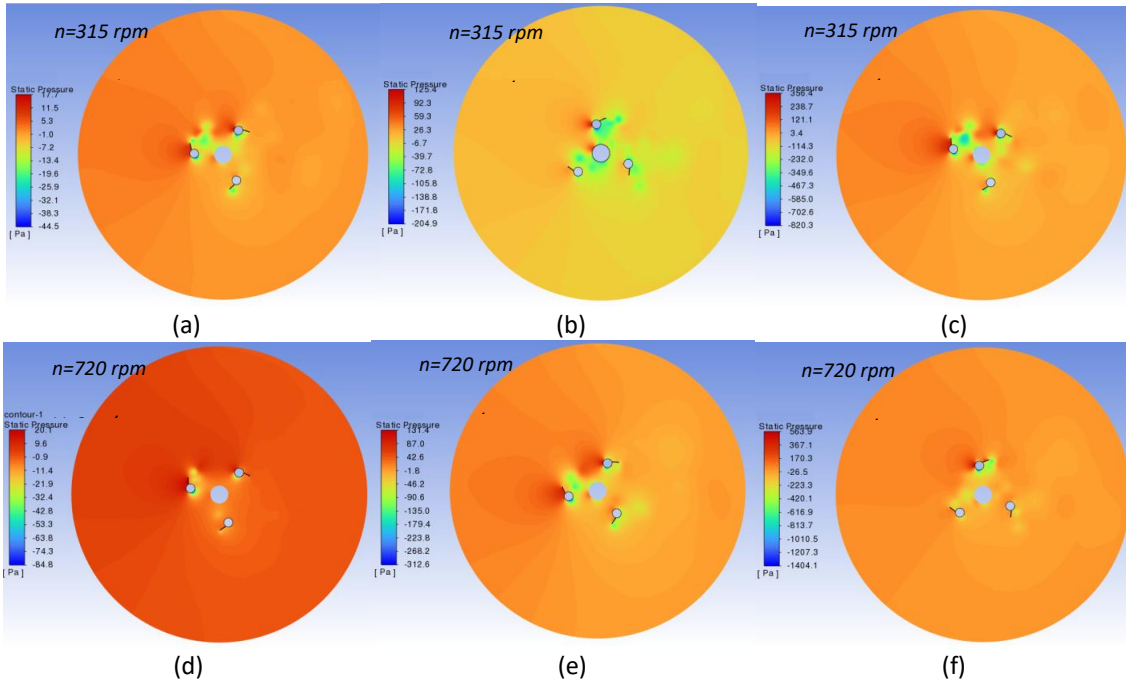


**Fig. 4.** Overpressure field: (a), (b), (c) –  $n=315$  rpm, (d), (e), (f) –  $n=720$  rpm, (a), (d) –  $V=3$  m/s, (b), (e) –  $V=9$  m/s, (c), (f) –  $V=15$  m/s

Table 2 shows the change in the pressure drop (the difference between the maximum and minimum overpressure) on the structural elements of the wind wheel.

**Table 2**  
 Pressure drops on the structural elements of the wind wheel, Pa.

	3 m/s	9 m/s	15 m/s
315 rpm	62	330	1177
550 rpm	75	370	1541
720 rpm	105	444	1968

The calculation results show, Figure 4, that to the left of the cylinders, blades and supports, the pressure is increased due to the air flow running into them. In the vicinity of the wind wheel, areas with reduced pressure are formed, caused by the disruption of vortices from the blades of the wind wheel.

From Figure 4, it is determined that areas with a high-pressure value are formed in the front of the cylinders and areas of low pressure are formed behind the cylinders. The separation of vortices behind the cylinders near the midsection is observed. An asymmetric pressure distribution is observed. In zones where the pressure has a maximum value, the flow velocity has a minimum value and vice versa, where the pressure is minimal in those zones, the velocity is maximum, which obeys the Bernoulli equation.

The results of the aerodynamic coefficients from the Reynolds number are presented below (Figure 5).

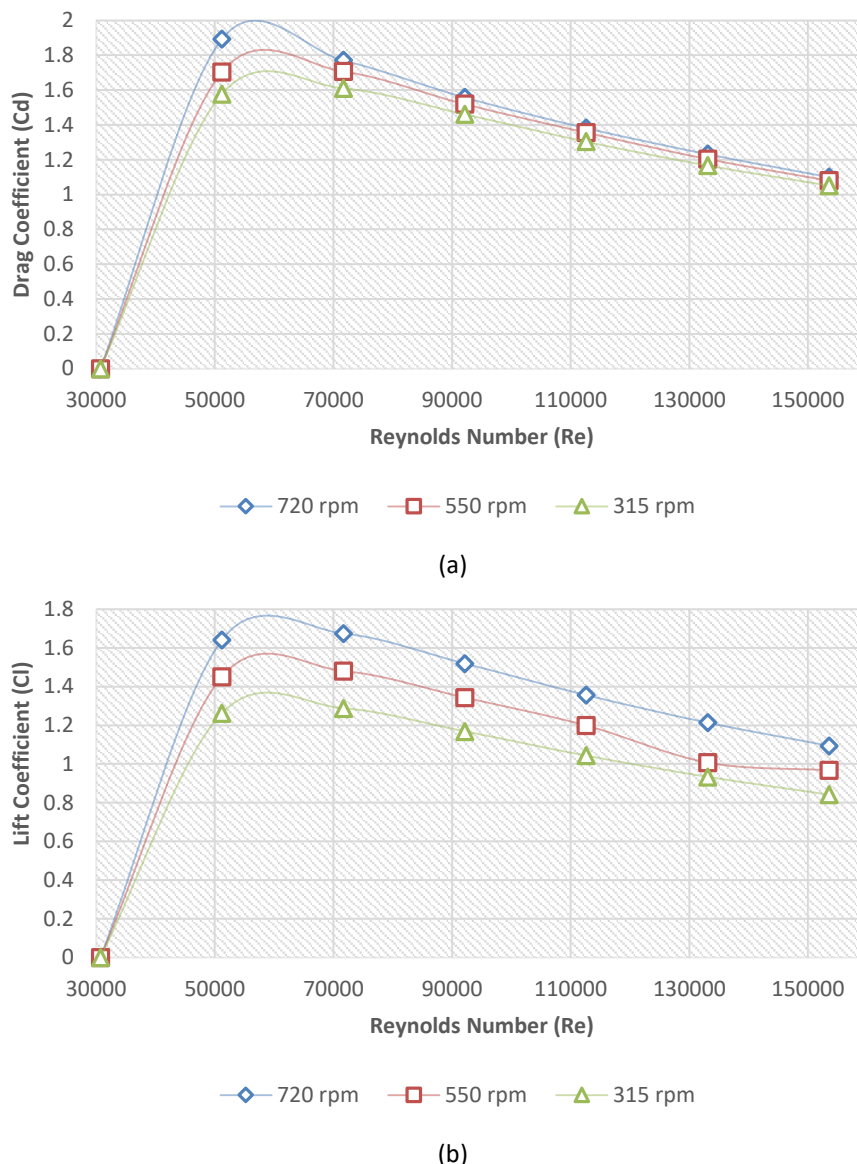


**Fig. 5.** Dependence of aerodynamic coefficients on the Reynolds number: a) coefficient of drag force; b) coefficient of lift

Figure 5(a) and 5(b) show the change in coefficients depending on the Reynolds number for a wind turbine with rotating cylindrical blades at different rotational speeds: 315, 550 and 720 rpm. In the Reynolds number range from 30,000 to 50,000, the drag coefficient increases rapidly, reaching maximum values of about 1.8 for 720 rpm, 1.6 for 550 rpm and 1.4 for 315 rpm. This peak indicates a transient flow regime, accompanied by increased vortex formation and flow separation. The maximum values of  $C_l$  are observed at  $Re \approx 50,000-60,000$ , while the highest value (about 1.75) is reached at 720 rpm, at 550 rpm — about 1.6 and at 315 rpm — about 1.4. After the peak value,  $C_l$  begins to decrease and at  $Re \approx 150,000$  its value decreases up to 0.8–1.0. The increase in lift to the peak is due to the favourable development of the boundary layer around the cylinder, which provides better aerodynamic characteristics. The addition of a fixed blade has a positive effect on reducing the drag coefficient of the  $C_d$ . Due to the stabilization of the flow and reduction of vortex formation behind the rotating cylinders, the  $C_d$  coefficient decreases by 10-15% in the range of high values of the Reynolds number. This results in a more streamlined flow and a reduction in the overall aerodynamic load on the turbine.

Numerical studies of the influence of the azimuth angle (from 0° to 50°) of the blade on the output values of aerodynamic coefficients at a maximum wind speed of 15 m/s were also carried out. This allows us to assess how a change in the position of the blade relative to the wind affects the coefficients of lift (Cl) and resistance (Cd), which is important for optimizing the operation of the wind turbine.

The dependences of the aerodynamic coefficients on the azimuth angle are shown below (Figure 6).

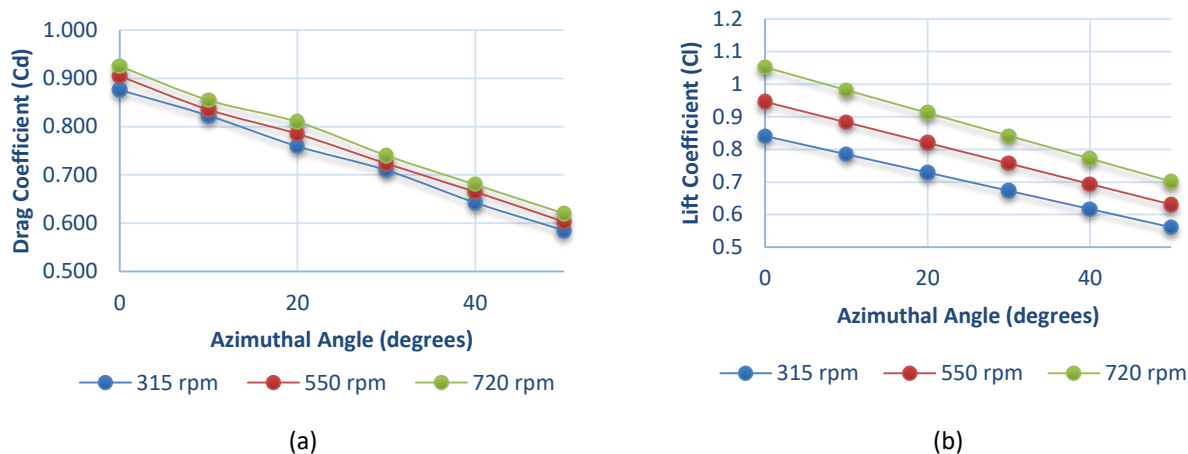


**Fig. 6.** The dependence of the aerodynamic coefficients on the azimuth angle: a) the coefficient of resistance (Cd) and b) the coefficient of lift.

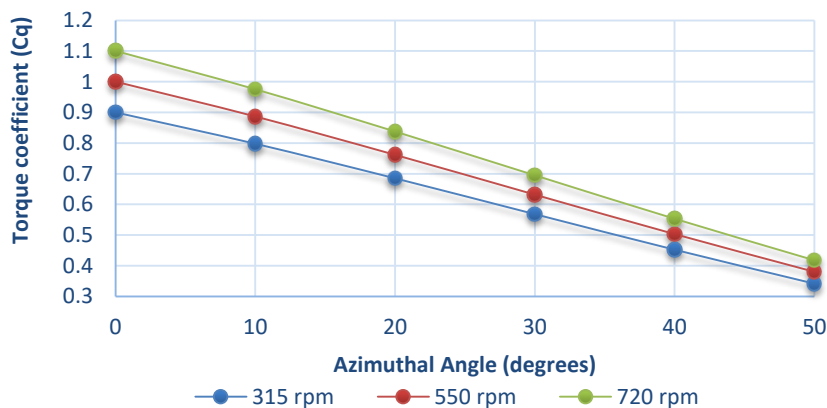
Figure 6(a) shows how the coefficient of resistance (Cd) changes with increasing azimuth angle at different rotational speeds: 315 rpm, 550 rpm and 720 rpm. It can be seen that with an increase in the angle from 0° to 50°, the coefficient of resistance gradually decreases for all rotational speeds. At an azimuthal angle of 0°, the Cd value is approximately the same for all three rotational speeds, being in the range of 0.88–0.9. As the angle increases, for example, at 50°, Cd decreases to values of about 0.6–0.7, with the lowest value observed at a rotational speed of 315 rpm. This decrease in the line is due to a change in the direction of the air flow relative to the surface of the blade, which reduces the impact of counter resistance.

Figure 6(b) shows how the lift coefficient (Cl) changes with increasing azimuth angle for the same rotational speeds. For all rotational speeds, Cl decreases with increasing angle from 0° to 50°. The highest Cl value is observed at 0° and a speed of 720 rpm (about 1.1), while the minimum value (about 0.6) is at 50° and 315 rpm. A decrease in the lift coefficient with an increase in the azimuth angle is associated with a change in the direction of the relative wind, which affects the aerodynamic behaviour of the blades and reduces their ability to generate lift.

It has been found that the lift coefficient is more sensitive to changes in rotation speed compared to the drag coefficient. The explanation for this is that the lift coefficient depends on the pressure drop, which increases with increasing cylinder rotation speed. This leads to a greater change in the lifting force compared to the resistance, which is determined by the counteraction of the flow and is less affected by the speed of rotation.

Below is a graph of the dependence of the torque coefficient (Cq) on the azimuth angle. The torque coefficient characterizes the ability of the blade to transfer the rotational force generated by the airflow to the turbine shaft. It depends both on the aerodynamic properties of the blade and on the angle of its position relative to the flow direction.

Below is a graph of the dependence of the torque coefficient (Cq) on the azimuth angle (Figure 7).



**Fig. 7.** Dependence of the torque coefficient ( $C_q$ ) on the azimuth angle

From Figure 7, the highest torque coefficient is observed at 720 rpm, starting from a value of about 1.1 at an angle of  $0^\circ$ . As the azimuth angle increases, the torque coefficient gradually decreases for all rotational speeds, reaching minimum values of about 0.4–0.5 at  $50^\circ$ . A decrease in the torque coefficient with an increase in the azimuth angle is associated with a change in the direction of the thrust force generated by the blade relative to the wind flow. At a higher angle, the blade is in a less favourable position to create torque due to the lower impact of the airflow on its surface. An increase in rotation speed leads to greater circulation and lift, which explains the higher  $C_q$  values for 720 rpm compared to other speeds.

Each wind turbine is characterized by a dimensionless value of the power coefficient ( $C_p$ ) [23], which is directly proportional to the resulting mechanical power on the shaft of the wind wheel and inversely proportional to the power of the incoming air flow.

The obtained results of calculating the power coefficient depending on the tip speed ratio ( $\lambda$ ) are shown in Figure 8.

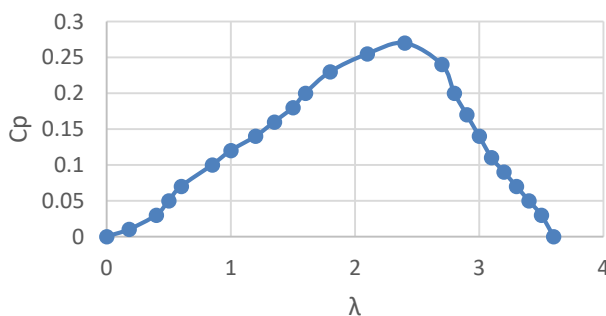


**Fig. 8.** Dependence of the power coefficient on the tip speed ratio

As can be seen from Figure 8, the maximum power factor is observed in the considered wind speed ranges from 3 to 15 m/s  $C_p = 0.27$  with the ratio of rotation speed to wind speed  $\lambda = 2.4$ . This value is in good agreement with the results presented by Libii [22] and is in the typical range for wind turbines with a vertical axis of rotation (VAWT). Although the maximum observed value corresponds to practical expectations, the shape of the curve  $\lambda$  shows some non-standard characteristics, especially at low values  $\lambda$ . These discontinuities may be related to the aerodynamic design and behaviour of the turbine under study, such as the effect of a fixed blade used to optimize the airflow around the blades.

According to Betz's Law [24], which establishes the theoretical limit for the power coefficient at 0.593, practical power coefficients for horizontal-axis wind turbines (HAWTs) reach up to 0.4, while vertical-axis turbines have maximum values around 0.38. Our design shows an initial increase in  $C_p$  with the growth of  $\lambda$  up to a peak value, confirming the high potential of the proposed design. This approach allows for a significant increase in wind energy utilization efficiency and demonstrates stable performance.

When comparing our combined blade wind turbine design with a traditional Magnus turbine equipped with only simple cylindrical blades without a fixed plate, a significant increase in the  $C_p$  power factor was found. As a result of numerical modelling, it was found that the addition of a fixed blade to a rotating cylinder leads to an increase in  $C_p$  by 1.5–1.7 times compared with the basic model without a fixed blade [25-27]. For a turbine with simple cylindrical blades, the power factor was  $C_p = 0.16-0.18$ , whereas for our improved design with an added fixed blade,  $C_p$  reached a value of 0.27. This indicates a positive effect of the fixed blade on the aerodynamic characteristics of the turbine. This phenomenon is due to a decrease in flow disruptions while vortex formation behind the rotating cylinder due to the addition of a fixed blade. This leads to an increase in lift and a decrease in drag force, which together improves the efficiency of converting wind energy into mechanical turbine energy.

The results of our numerical simulation are based on previously conducted experimental studies published in a separate paper that studied the aerodynamic characteristics of wind turbine blades with the addition of fixed plates. Experimental data confirmed [28] an improvement in lift and a decrease in drag due to a decrease in vortex formation, which corresponds to the numerical results obtained. This relationship between numerical and experimental results emphasizes the reliability of the presented conclusions and demonstrates the effectiveness of the proposed design in real operating conditions. In the future, it is planned to integrate data from numerical and experimental studies to further optimize the design and increase its efficiency.

In this paper, the main attention is paid to the effect of adding a fixed blade and analysing the results depending on the azimuth angle, which made it possible to evaluate the efficiency of the turbine under certain conditions. However, further investigation of various design options and configurations could expand the understanding of possible ways to optimize and improve turbine performance.

#### 4. Conclusions

During the numerical simulation of a wind turbine with combined blades:

- i. a model of an installation with combined blades was created and the Realizable k- $\epsilon$  model was chosen as the turbulence model;
- ii. the results of the current line in the immediate vicinity of the wind wheel and the overpressure field at 3.9.15 m/s and at rotational speeds of 315, 550 and 720 rpm were obtained. Based on the analysis of the flow visualization results, the flow modes of the cylinder are distinguished, which differ in the nature of the formation of large-scale vortex structures. It is determined that a force (lifting) acts on each blade, which is perpendicular to the axis of the blade and the direction of the wind. Since all the blades rotate in the same direction around their axis, the lifting force creates a moment of force that causes the wind wheel to rotate clockwise;

- iii. it is determined that the addition of a fixed blade to the cylinder increases the power factor of the wind turbine by almost 1.5-1.7 times, which ultimately increases the efficiency of the entire installation.

To further improve the efficiency of Magnus wind turbines, additional design and configuration modifications should be considered in future studies. This may include testing different blade shapes, using advanced flow control mechanisms or combining fixed and movable blade elements. Such studies will help to better understand the potential for improvements and expand the possibilities of optimizing the characteristics of Magnus turbines.

Future work should also include experimental verification of these numerical results to improve the reliability of the conclusions. This may include the development of a prototype based on a numerical model and the conduct of controlled tests to confirm the practical applicability and improvements in the characteristics indicated in the simulations.

### Acknowledgement

This research was funded by a grant from Science Committee of the Ministry of Science and Higher Education of the Republic of Kazakhstan (AP22785282 "Automation process detecting errors and improving efficiency operation compact combined power plant based on solar panels and wind generators").

### References

- [1] International Energy Agency. "Wind." *International Energy Agency*, (2022). <https://www.iea.org/energy-system/renewables/wind>
- [2] Shah, Sahishnu R., Rakesh Kumar, Kaamran Raahemifar and Alan S. Fung. "Design, modeling and economic performance of a vertical axis wind turbine." *Energy Reports* 4 (2018): 619-623. <https://doi.org/10.1016/j.egyr.2018.09.007>
- [3] Manganhar, Abdul Latif, Altaf Hussain Rajpar, Muhammad Ramzan Luhur, Saleem Raza Samo and Mehtab Manganhar. "Performance analysis of a savonius vertical axis wind turbine integrated with wind accelerating and guiding rotor house." *Renewable Energy* 136 (2019): 512-520. <https://doi.org/10.1016/j.renene.2018.12.124>
- [4] Alrowwad, Ibrahim, Xiaojia Wang and Ningling Zhou. "Numerical modelling and simulation analysis of wind blades: a critical review." *Clean Energy* 8, no. 1 (2024): 261-279. <https://doi.org/10.1093/ce/zkad078>
- [5] Alizadeh, Hossein, Mohammad Hossein Jahangir and Roghayeh Ghasempour. "CFD-based improvement of Savonius type hydrokinetic turbine using optimized barrier at the low-speed flows." *Ocean Engineering* 202 (2020): 107178. <https://doi.org/10.1016/j.oceaneng.2020.107178>
- [6] Sewucipto, Sanjaya and Triyogi Yuwono. "The influence of upstream installation of D-53° type cylinder on the performance of Savonius turbine." *Journal of Advanced Research in Experimental Fluid Mechanics and Heat Transfer* 3, no. 1 (2021): 36-47.
- [7] Salleh, Mohd Badrul, Noorfazreena M. Kamaruddin and Zulfaa Mohamed-Kassim. "The effects of deflector longitudinal position and height on the power performance of a conventional Savonius turbine." *Energy Conversion and Management* 226 (2020): 113584. <https://doi.org/10.1016/j.enconman.2020.113584>
- [8] Saad, Ahmed S., Ibrahim I. El-Sharkawy, Shinichi Ookawara and Mahmoud Ahmed. "Performance enhancement of twisted-bladed Savonius vertical axis wind turbines." *Energy Conversion and Management* 209 (2020): 112673. <https://doi.org/10.1016/j.enconman.2020.112673>
- [9] Li, Shoutu, Ye Li, Congxin Yang, Qiang Wang, Bin Zhao, Deshun Li, Ruiwen Zhao *et al.*, "Experimental investigation of solidity and other characteristics on dual vertical axis wind turbines in an urban environment." *Energy Conversion and Management* 229 (2021): 113689. <https://doi.org/10.1016/j.enconman.2020.113689>
- [10] Yan, Yan, Eldad Avital, John Williams and Jiahuan Cui. "Aerodynamic performance improvements of a vertical axis wind turbine by leading-edge protuberance." *Journal of Wind Engineering and Industrial Aerodynamics* 211 (2021): 104535. <https://doi.org/10.1016/j.jweia.2021.104535>
- [11] Bakhtybekova, Asem Ravshanbekovna, Nazgul'Kadyralievna Tanasheva, Leonid Leonidovich Minkov, Nurgul Nayzabekovna Shuyushbayeva and Ainura Nurtaevna Dyusembaeva. "Aerodynamic features of a rotating cylinder

- with a deflector." *Journal of Applied Mechanics and Technical Physics* 63, no. 5 (2022): 833-842. <https://doi.org/10.1134/S0021894422050121>
- [12] Dyusembaeva, A. N., A. Zh Tleubergenova, N. K. Tanasheva, B. R. Nussupbekov, A. R. Bakhtybekova and Sh S. Kyzdarbekova. "Numerical investigation of the flow around a rotating cylinder with a plate under the subcritical regime of the Reynolds number." *International Journal of Green Energy* 21, no. 5 (2024): 973-987. <https://doi.org/10.1080/15435075.2023.2228394>
- [13] Klimina, L. A. "Darrieus-magnus type wind turbine: Dynamics and control." *Journal of Computer and Systems Sciences International* 60 (2021): 756-769. <https://doi.org/10.1134/S1064230721050129>
- [14] Zhao, Ming. "A review of recent studies on the control of vortex-induced vibration of circular cylinders." *Ocean Engineering* 285 (2023): 115389. <https://doi.org/10.1016/j.oceaneng.2023.115389>
- [15] Bahambary, Khashayar Rahnamay and Brian Fleck. "A study of inflow parameters on the performance of a wind turbine in an atmospheric boundary layer." *Journal of Advanced Research in Numerical Heat Transfer* 11, no. 1 (2022): 5-11.
- [16] Eydi, Faezeh and Afsaneh Mojra. "A numerical study on the benefits of passive-arc plates on drag and noise reductions of a cylinder in turbulent flow." *Physics of Fluids* 35, no. 8 (2023). <https://doi.org/10.1063/5.0156197>
- [17] Kimura, Yusuke and Shigeru Ogawa. "Study on wingtip vortices of vertical axis type Magnus wind turbine." In *Grand Renewable Energy proceedings Japan council for Renewable Energy (2018)*, p. 182. Japan Council for Renewable Energy, 2018.
- [18] Sedaghat, Ahmad, Iman Samani, Mojtaba Ahmadi-Baloutaki, M. El Haj Assad and Mohamed Gaith. "Computational study on novel circulating aerofoils for use in Magnus wind turbine blades." *Energy* 91 (2015): 393-403. <https://doi.org/10.1016/j.energy.2015.08.058>
- [19] Marzuki, O. F., A. M. Rafie, F. I. Romli and K. A. Ahmad. "An experimental investigation on the effect of surface roughness on the performance of Magnus wind turbine." *ARPJ. Eng. Appl. Sci* 10, no. 20 (2015): 9725-9729.
- [20] Cherif, Hakima, Abderrahmane Khechekhouche, Madiha Maamir, Hania Aboub and Basim Belgasim. "Modelling and Control of a Small Domestic Wind Turbine." *ASEAN Journal of Science and Engineering* 3, no. 2 (2023): 115-122. <https://doi.org/10.17509/ajse.v3i1.44725>
- [21] Limpot, Harriet Elaine, Alyssa Somido, Angela Shayne Yamsuan, Binoe E. Abuan and Louis Angelo M. Danao. "The performance of a Magnus vertical axis wind turbine in typhoon wind speeds." *Chemical Engineering Transactions* 103 (2023): 181-186.
- [22] Libii, Josué Njock. "Comparing the calculated coefficients of performance of a class of wind turbines that produce power between 330 kW and 7,500 kW." *World Transactions on Engineering and Technology Education* 11, no. 1 (2013): 36-40.
- [23] Tanasheva, N. K., A. R. Bakhtybekova, N. N. Shuyushbayeva, A. K. Tussupbekova and A. Zh Tleubergenova. "Calculation of the aerodynamic characteristics of a wind-power plant with blades in the form of rotating cylinders." *Technical Physics Letters* 48, no. 2 (2022): 51-54. <https://doi.org/10.1134/S1063785022020092>
- [24] Kolganov, A. V., V. A. Zemlyanovskiy, Ch S. Guseinov and N. N. Portnyagin. "Submersible power-generating unit as an alternative energy sources." In *IOP Conference Series: Materials Science and Engineering*, vol. 1201, no. 1, p. 012006. IOP Publishing, 2021. <https://doi.org/10.1088/1757-899X/1201/1/012006>
- [25] Lukin, Aleksandr, Galina Demidova, Anton Rassõlkin, Dmitry Lukichev, Toomas Vaimann and Alecksey Anuchin. "Small Magnus wind turbine: Modeling approaches." *Applied Sciences* 12, no. 4 (2022): 1884. <https://doi.org/10.3390/app12041884>
- [26] Richmond-Navarro, Gustavo, Williams R. Calderón-Munoz, Richard LeBoeuf and Pablo Castillo. "A Magnus wind turbine power model based on direct solutions using the Blade Element Momentum Theory and symbolic regression." *IEEE Transactions on sustainable energy* 8, no. 1 (2016): 425-430. <https://doi.org/10.1109/TSTE.2016.2604082>
- [27] Tanasheva, N. K., A. R. Bakhtybekova, K. M. Shaimerdenova, S. E. Sakipova and N. N. Shuyushbayeva. "Correction to: Modeling Aerodynamic Characteristics of a Wind Energy Installation with Rotating Cylinder Blades on the Basis of the Ansys Suite." *Journal of Engineering Physics and Thermophysics* 95, no. 3 (2022): 846-846. <https://doi.org/10.1007/s10891-022-02542-7>
- [28] Tanasheva, N. K., A. R. Bakhtybekova, N. N. Shuyushbayeva, A. N. Dyusembaeva, M. A. Burkov and S. A. Nurkenov. "Experimental study of aerodynamic coefficients of a combined blade." *Bulletin of the Karaganda University" Physics Series"* 11329, no. 1 (2024): 92-98. <https://doi.org/10.31489/2024ph1/92-98>